

Vibration analysis thermally affected viscoelastic nanosensors subjected to linear varying loads

Farzad Ebrahimi^{*}, Ramin Babaei and Gholam Reza Shaghaghi

*Department of Mechanical Engineering, Faculty of Engineering,
Imam Khomeini International University, Postal code: 3414916818, Qazvin, Iran*

(Received August 23, 2018, Revised November 16, 2018, Accepted November 22, 2018)

Abstract. Unwanted vibration is an issue in many industrial systems, especially in nano-devices. There are many ways to compensate these unwanted vibrations based on the results of the past researches. Elastic medium and smart material etc. are effective methods to restrain unnecessary vibration. In this manuscript, dynamic analysis of viscoelastic nanosensor which is made of functionally graded (FGM) nanobeams is investigated. It is assumed that, the shaft is flexible. The system is modeled based on Timoshenko beam theory and also environmental condition, external linear varying loads and thermal loading effect are considered. The equations of motion are extracted by using energy method and Hamilton principle to describe the translational and shear deformation's behavior of the system. Governing equations of motion are extracted by supplementing Eringen's nonlocal theory. Finally vibration behavior of system especially the frequency of system is developed by implementation Semi-analytical differential transformed method (DTM). The results are validated in the researches that have been done in the past and shows good agreement with them.

Keywords: nanosensor; dynamic analysis; functionally graded material; viscoelastic material; linear varying loads; thermal loading effects; Eringen nonlocal theory

1. Introduction

Nanosensors are devices for measuring physical-chemical changes and convert into understandable signals for humans. These sensors respond the specific reactions that are foreseen to them beforehand. In all of these nanosensors, a substance is always in contact with the study environment. The task of this substance is to detect changes in the study environment. The accuracy of the sensor, response speed, dismissing the impact of disturbing environment and power of choice are examples of important parameters in nanosensors.

Nanosensors are included nanotubes, nanodevices, quantum nanosensors and etc. quantum nanosensors consist of semiconductor crystals and transmits the information by attracting optical magnetic fields and converting them into expected wavelengths. These sensors are used in optical devices but nanotubes are derived from the novel material such as carbon, ceramic, metal and etc. composites. These nanotubes have wide applications such as identifying low concentration –high speed material, detection of gas molecules at low concentration and etc.

^{*}Corresponding author, Ph.D., E-mail: febrahimi@eng.ikiu.ac.ir

There are many studies about nanostructure with consideration of thermal effect (Ebrahimi and Shaghghi 2016), “buckling (Ebrahimi *et al.* 2014, 2016b, 2018) vibration (Ebrahimi *et al.* 2014, 2018, Ghadiri *et al.* 2015, Ebrahimi *et al.* 2015), nonlinear vibration (Ebrahimi and Shaghghi 2018), “wave propagation (.....), “nanosensors (Duan *et al.* 2018) and dynamics of nanostructure (Zhu and Li 2017).

Also there are kinds of size-dependent continuum theories like couple stress elasticity theory (Zhou *et al.* 2018), “strain gradient theory (Li and Hu 2017), “nonlocal strain gradient theory (.....) and modified couple stress theory which are announced to consider the size effect.

FG materials are one of the novel composites that have continuously varying material composition and properties through certain dimension (thickness direction) of the structure to achieve the desired goals. As the fiber-reinforced composites have mismatch material. In functionally graded materials, ceramics are used to improve thermal properties and metals are used to improve strength properties. Method of placement and amount of each of these materials determines the rates and mode of mechanical properties' changes in the structure. The nonlinear vibration of shear deformable FGM carbon nanotube which is reinforced by composite based on the first-order shear deformation beam theory and von Kármán geometric nonlinearity is studied by Wu *et al.* (2016), “In other work, Fernandes and his colleagues presented the response of single-walled carbon nanotube's (CNT) longitudinal linear and nonlinear free vibration which is embedded in an elastic medium and subjected to boundary conditions (Fernandes *et al.* 2017), “Ebrahimi and Farazmand Nia proposed a higher-order shear deformation beam theory (HSBT) for analysis of functionally graded carbon nanotube's (FG-CNTRC) free vibration. This study has been done on sandwich beams and thermal effects are considered (Ebrahimi and Farazmand 2017), “In other research work, the influences of critical speed on the spinning 3D single-walled carbon nanotubes (SWCNT) free vibration behavior are investigated by Ghadiri *et al.* (2015), “Ansari *et al.* (2016) established a nonlinear fractional nonlocal Euler-Bernoulli beam model by using the concept of fractional derivative and also nonlocal elasticity theory to investigate the size-dependent geometrically nonlinear free vibration of fractional viscoelastic nanobeams. The effect of non-local higher order stress on the nonlinear vibration of carbon nanotube (CNT) conveying viscous nanoflow resting on the elastic foundation is investigated by Mohammadimehr *et al.* (2017).

There are many other research activities on the vibration of mechanical structures, for example, Murmu and Adhikari (2013) developed a single layer graphene sheets (SLGS) mass sensor by considering nonlocal elasticity incorporates the small scale effects or in other words nonlocality. In a study, Karličić *et al.* (2015) used the nonlocal Kirchhoff-Love plate theory to describe single-layered graphene sheet's mechanical behavior as an orthotropic nanoplate. Arda and Aydogdu (2017) investigated the longitudinal vibration of a carbon nanotube with an attached damper by accomplishing the nonlocal stress gradient elasticity theory. Li *et al.* (2015) are studied free vibration and mass detection of carbon nanotube-based sensors. In this paper exact equations for the resonance frequencies of nanoscale resonators are derived, explicit expressions for calculating the fundamental frequencies are provided and formulae for identifying attached mass are established. The theoretical framework for a single-walled carbon nanotube serving as a virus or bacterium sensor, with the complicating influences of non-locality and considering surface effects developed by Elishakoff *et al.* (2013), “Hwang and his colleagues examined brake friction materials containing multi-wall carbon nanotubes (CNTs) to determine their effect on the braking performance (Hwang *et al.* 2010), “Ebrahimi *et al.* examined thermo-mechanical buckling problem of functionally graded (FG) nanoplates supported by Pasternak elastic foundation subjected to

linearly/non-linearly varying loadings is analyzed via the nonlocal elasticity theory (Ebrahimi *et al.* 2016a, b, Ebrahimi and Barati 2016a-j)

In this manuscript, dynamic analysis of FGM nanosensor subjected to various linear and non-linear varying normal in-plane forces and resting on Pasternak foundation with intrinsic viscoelastic properties are investigated for the first time. Thermal effects and surface effects are also considered. Nanosensor is modeled based on Timoshenko beam theory. Nonlocal elasticity theory and Hamilton's principle are utilized to extract the governing equations and the DTM's method is applied to solve them. The presented shows a good agreement with the results available in literature. The small size effect on the vibration behaviors of functionally graded rectangular nanobeams is presented through considering various parameters such as FG-index, the length of nanoplates, numerical loading factor, nonlocal parameter, aspect ratio and the mode numbers.

2. Formulation

2.1 Nonlocal theory

The constitutive equation of classical elasticity is an algebraic relationship between the stress and strain tensors while that of Eringen's nonlocal elasticity involves spatial integrals which represent weighted averages of the contributions of strain tensors of all points in the body to the stress tensor at the given point (Eringen 1983), "Though it is difficult mathematically to obtain the solution of nonlocal elasticity problems due to the spatial integrals in constitutive equations, these integro-partial constitutive differential equations can be converted to equivalent differential constitutive equations under certain conditions.

The theory of nonlocal elasticity, developed by Eringen and Edelen (1972) states that the nonlocal stress-tensor components σ_{ij} at any point x in a body can be expressed as

$$\sigma_{ij}(x) = \int_{\Omega} \left(\alpha(|x' - x|, \tau) t_{ij}(x') \right) d\Omega(x') \quad (1)$$

where $t_{ij}(x')$ are the components of the classical local stress tensor at point x , which are related to the components of the linear strain tensor ε_{kl} by the conventional constitutive relations for a Hookean material, i.e.

$$t_{ij} = C_{ijkl} \varepsilon_{kl} \quad (2)$$

The meaning of Eq. (1) is that the nonlocal stress at point x is the weighted average of the local stress of all points in the neighborhood of x , the size of which is related to the nonlocal Kernel $\alpha(|x' - x|, \tau)$. Here $|x' - x|$ is the Euclidean distance and τ is a constant given by

$$\tau = \frac{e_0 a}{l} \quad (3)$$

Which represents the ratio between a characteristic internal length, a (such as lattice parameter, C-C bond length and granular distance) and a characteristic external one, l (e.g., crack length, wavelength) through an adjusting constant, e_0 , dependent on each material. The magnitude of e_0 is

determined experimentally or approximated by matching the dispersion curves of plane waves with those of atomic lattice dynamics. According to (Eringen and Edelen 1972) for a class of physically admissible kernel $\alpha(|x' - x|, \tau)$ it is possible to represent the integral constitutive relations given by Eq. (1) in an equivalent differential form as

$$(1 - (e_0 a) \nabla^2) \sigma_{kl} = t_{kl} \quad (4)$$

In which ∇^2 is the Laplacian operator. Thus, the scale length $e_0 a$ takes into account the size effect on the response of nanostructures. For an elastic material in the one dimensional case, the nonlocal constitutive relations may be simplified as (Miller and Shenoy 2000)

$$\sigma_{xx} - \mu \frac{\partial^2 \sigma_{xx}}{\partial x^2} = E \varepsilon_{xx} \quad (5)$$

Where σ and ε are the nonlocal stress and strain respectively, $\mu = (e_0 a)^2$ is the nonlocal parameter and E is the elasticity modulus (Ebrahimi *et al.* 2016a, b, c, d), "Parameter of $e_0 a$ can be vary among 0 to 5 nm which $e_0 a = 0$ equals to classical continuum theory.

2.2 Functionally graded nanobeam

As depicted in Fig. 1, an FGM nanosensor of length l_x and thickness h that is made of a mixture of ceramics and metals is considered. It is assumed that the materials at bottom surface ($Z = -h/2$) and the top surface ($Z = h/2$) of the nanoplate are metals and ceramics, respectively. The local effective material properties of an FGM nanobeam can be calculated using homogenization method that is based on the Mori–Tanaka scheme. According to the Mori–Tanaka homogenization technique, the effective material properties of the FGM nanobeam such as Young's modulus (E), "Poisson's ratio (ν), "mass density (ρ) and thermal extension coefficient (α) can be determined as follows (Mori and Tanaka 1973)

$$E(z) = E_c V_c(z) + E_m V_m \quad (6a)$$

$$\rho(z) = \rho_c V_c(z) + \rho_m V_m \quad (6b)$$

$$\alpha(z) = \alpha_c V_c(z) + \alpha_m V_m \quad (6c)$$

$$\nu(z) = \nu_c V_c(z) + \nu_m V_m \quad (6d)$$

Here, the subscripts m and c refer to metal and ceramic phases. The volume fraction of the ceramic and metal phases can be defined by the power-law function as

$$V_f(z) = \left(\frac{1}{2} + \frac{z}{h} \right)^k \quad (7)$$

Where k represents the power-law index. Additionally, the neutral axis of FGM nanobeam where the end supports are located on, can be determined by the following relation

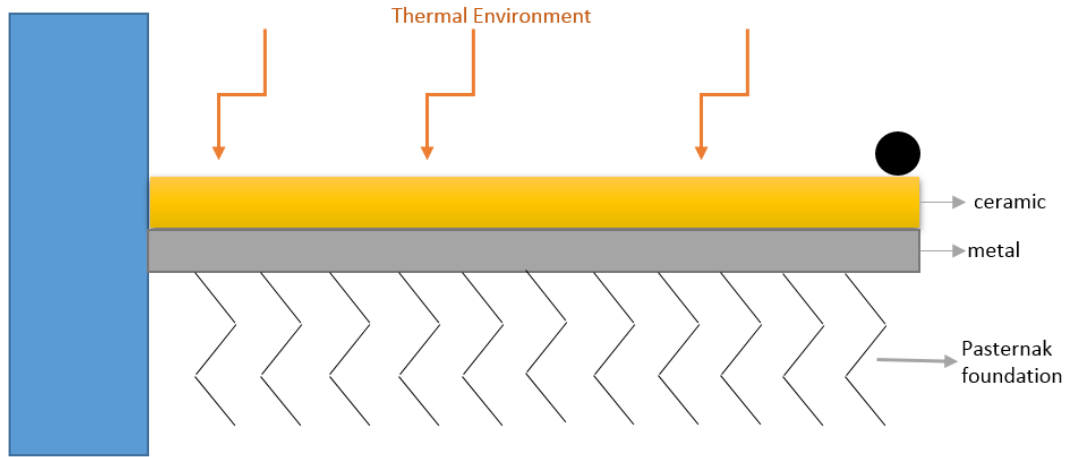


Fig. 1 Schematic view of functionally graded nanosensor

$$z_0 = \frac{\int_{-(h/2)}^{(h/2)} zE(z)dz}{\int_{-(h/2)}^{(h/2)} E(z)dz} \tag{8}$$

2.3 Governing equation

u and w , are component of displacement's field of an arbitrary point in the mid-plane along the x and z directions, respectively. According to the Timoshenko beam theory, the displacement field can be presented as

$$u_x(x, z, t) = u(x, t) + z\varphi(x, t), \quad u_z(x, z, t) = w(x, t) \tag{9}$$

U and W , are the displacement components of an arbitrary point (x, z) at a distance z from the middle of the plate thickness in the x and z directions, respectively. The strain-displacement relationships are presented following strain field. These equations are independent of constitutive equations. The tensorial strain field can be shown as

$$\varepsilon_{xx} = \varepsilon_{xx}^0 + zk^0, \quad \varepsilon_{xx}^0 = \frac{\partial u(x, t)}{\partial x}, \quad k^0 = \frac{\partial \varphi(x, t)}{\partial x} \tag{10a}$$

$$\gamma_{xz} = \frac{\partial w(x, t)}{\partial x} + \varphi(x, t) \tag{10b}$$

In which, ε_{xx}^0 and k^0 represent the strain on the middle plane and curvature respectively. The nanobeam is made of frictional viscoelastic material. The frictional viscoelastic nanobeams are modeled based on the Kelvin-Voigt theory as follows

$$\sigma_{xx} = E \left(1 + g \frac{\partial^\alpha}{\partial t^\alpha} \right) \varepsilon_{xx} \tag{11}$$

According to this theory, the main axial stresses σ_{xx} is not just function of the elastic modulus but also the viscoelastic coefficient g and frictional order α also effect it. Frictional order always has a value between 0 and 1 and is extracted individually from the following function (Ansari *et al.* 2016)

$$D_t^\alpha(w) = I^{1-\alpha}(\dot{w}) = \frac{1}{\Gamma(1-\alpha)} \int_0^t \frac{w'(t-\tau)}{\tau^\alpha} d\tau + \frac{w(0)}{\Gamma(1-\alpha)t^\alpha} \quad (12)$$

The effect of surface stresses on the behavior of system based on Gurtin-Murdoch theory can be represents as follows

$$\tau_{\alpha\beta}^{sl} = \tau_{\alpha\beta}^0 + C_{\alpha\beta\gamma\delta}^s \varepsilon_{\gamma\delta} - e_{\alpha\beta k}^s E_k \quad (13)$$

In which, $\tau_{\alpha\beta}^0$ shows residual surface stresses at upper and downer surface of structure. $C_{\alpha\beta\gamma\delta}^s$ and $e_{\alpha\beta k}^s$ represents other coefficient of equation that are related to Lamé coefficient.

$$\tau_{xx} = \tau_0 + E^s u_{x,x}, \quad E^s = 2\mu_0 \lambda_0, \quad \tau_{zx} = \tau_0 u_{z,x} \quad (14)$$

Where μ_0 and λ_0 are Lamé coefficient which are related to surface properties. In the Gurtin-Murdoch theory one cannot negligible σ_{zz} so σ_{zz} is defined as follows

$$\sigma_{zz} = \frac{2z\nu}{h} \left(\tau_0 \frac{\partial^2 w}{\partial x^2} - \rho_0 \frac{\partial^2 w}{\partial t^2} \right) \quad (15)$$

Now, by using Hamilton principle

$$\int_0^t \delta(U - T + W_{ext}) dt = 0 \quad (16)$$

Where U , T and W_{ext} represents strain energy, kinetic energy and the work done by external forces respectively. First order variation of system's strain energy can be shown as

$$\delta U = \int_V \sigma_{ij} \delta \varepsilon_{ij} dV = \int_V (\sigma_{xx} \delta \varepsilon_{xx} + \sigma_{xx}^s \delta \varepsilon_{xx} + \sigma_{xz} \delta \gamma_{xz} + \sigma_{xz}^s \delta \gamma_{xz}) dV \quad (17)$$

By substituting strains obtained from strain-displacement relation it can be shown

$$\delta U = \int_0^L (N_x (\delta \varepsilon_{xx}^0) + M_x (\delta k^0) + Q (\delta \gamma_{xz})) dx \quad (18)$$

where N_x , M_x and Q are axial forces, bending moment and lateral forces, respectively that's defined as below

$$N = \int_A (\sigma_{xx} + \sigma_{xx}^s) dA, \quad M = \int_A (\sigma_{xx} + \sigma_{xx}^s) z dA, \quad (20)$$

$$Q = \int_A K_s (\sigma_{xz} + \sigma_{xz}^s) dA$$

The variation of kinetic energy of Timoshenko beam can be represents as

$$T = \frac{1}{2} \int_0^L \int_A \left[\rho(z) \left(\left(\frac{\partial u_x}{\partial t} \right)^2 + \left(\frac{\partial u_z}{\partial t} \right)^2 \right) + (\rho^s_{+h/2} + \rho^s_{-h/2}) \left(\frac{\partial u_z}{\partial t} \right)^2 \right] dA dx \quad (21)$$

First order variation of system's strain energy can be shown as

$$\begin{aligned} \delta T = \int_0^L \left[I_0 \left(\frac{\partial u}{\partial t} \frac{\partial \delta u}{\partial t} + \frac{\partial w}{\partial t} \frac{\partial \delta w}{\partial t} \right) + I_1 \left(\frac{\partial \varphi}{\partial t} \frac{\partial \delta u}{\partial t} + \frac{\partial u}{\partial t} \frac{\partial \delta \varphi}{\partial t} \right) + \right. \\ \left. I_2 \frac{\partial \varphi}{\partial t} \frac{\partial \delta \varphi}{\partial t} + (\rho^s_{+h/2} + \rho^s_{-h/2}) \frac{\partial w}{\partial t} \frac{\partial \delta w}{\partial t} \right] dx \end{aligned} \quad (22)$$

In which, (I_0, I_1, I_2) are mass moment which are defined as below

$$(I_0, I_1, I_2) = \int_A \rho(z) (1, z, z^2) dA \quad (23)$$

Variation of works done by external forces includes many terms but for physical loading it can be written as

$$\delta W_{ext} = \int_0^L (f(x) \delta u + q(x) \delta w) dx \quad (24)$$

In which, $f(x)$ and $q(x)$ represents work done by external load and linear varying loads along the length direction of beam. To modeling thermal environment and its effect on the behavior of system firstly need to define the thermal stresses as below

$$\sigma_x^T = \frac{E \alpha (T - T_0)}{I - \nu} \quad (25)$$

Where α and T_0 shows the thermal conductivity coefficient and ambient temperature. The temperature is Kelvin and the initial value is 300°. The work done by thermal stresses can be written as

$$W_{th} = \int_A \left[N_{Tx} \left(\frac{\partial w}{\partial x} \right)^2 \right] dA \quad (26)$$

In which

$$N_{Tx} = \int_{\left(\frac{h}{2}\right)}^{\left(-\frac{h}{2}\right)} \sigma_{Tx} dz \quad (27)$$

So the variation of work done by thermal stresses can be represent as

$$\delta W_{th} = \int_A \left[N_{Tx} \delta \left(\frac{\partial w}{\partial x} \right)^2 \right] dA \quad (28)$$

Pasternak medium is also modeled in the same way. This foundation is considered as a set of springs with coefficient K_G . The work done by displacement of springs can be written as

$$W_{pas} = \int_A \left[K_G \left(\frac{\partial w}{\partial x} \right)^2 \right] dA \quad (29)$$

And also the variation of works done by Pasternak medium's displacement can be written as

$$\delta W_{pas} = \int_A \left[K_G \delta \left(\frac{\partial w}{\partial x} \right)^2 \right] dA \quad (30)$$

The residual surface stresses can be considered as an external force. So the work done by residual surface stress can be shown as

$$W_{resi} = \int_A \left[2b \tau_0 \left(\frac{\partial w}{\partial x} \right)^2 \right] dA \quad (31)$$

And the variation of works done by residual surface stresses can be written as

$$\delta W_{resi} = \int_A \left[2b \tau_0 \delta \left(\frac{\partial w}{\partial x} \right)^2 \right] dA \quad (32)$$

To modeling the humidity of the environment and its effect on behavior of system will have the following relation

$$N^H = - \int_A E \beta \Delta H dA = -E \beta \Delta H dA \quad (33)$$

Where N^H and β shows the amount of humidity in arbitrary point and humidity coefficient respectively. The variation of works done by the humidity stresses can be written as

$$\delta W_{Nh} = \int_A \left[N_{Nh} \delta \left(\frac{\partial w}{\partial x} \right)^2 \right] dA \quad (34)$$

Modeling of the linear varying loading at the end of the beam and the along the thickness direction that are includes all types of loading from the simple pressure to pure bending can be represents as

$$q = -P_0 \left(1 - \chi \left(\frac{y}{l_y} \right) \right) \quad (35)$$

Where N^h and β shows the amount of humidity in arbitrary point and humidity coefficient respectively. The variation of works done by the humidity stresses can be written as

$$\delta W_{Nh} = \int_A \left[N_{Nh} \delta \left(\frac{\partial w}{\partial x} \right)^2 \right] dA \tag{36}$$

χ Specifies the amount of numerical loading factor. P_0 is the compressive force per unit length at $y = 0$. This in-plane force distribution is seen at the two nanoplates opposite edges ($x = 0, x = l_x$). χ 's change, shows different form of in-plane loadings. If $\chi = 0$, then the situation of uniform compressive force is investigated. If $\chi = 1$, the force decrease from $-P_0$ at $y = 0$, to zero at $y = l_y$ and if $\chi = 2$, we'll see pure bending. This type of modeling allows the full range of loads from pure compression to pure bending considered only on the basis of unit modeling. These different situations of loadings condition are shown in Fig. 2.

Bsed on Fundamental Lema and by separating the coefficients of $\delta u, \delta v$ and δw the following equation of motion are achieved

$$\frac{\partial N}{\partial x} + f = I_0 \frac{\partial^2 u}{\partial t^2} + I_1 \frac{\partial^2 \varphi}{\partial t^2} \tag{37}$$

$$\frac{\partial Q}{\partial x} + F = I \frac{\partial^2 w}{\partial t^2} \tag{38}$$

$$\frac{\partial M}{\partial x} - Q = I_1 \frac{\partial^2 u}{\partial t^2} + I_2 \frac{\partial^2 \varphi}{\partial t^2} \tag{39}$$

In which F and I defined as below

$$F = (q + 2b\tau_0 + K_G + N_{Tx} + N_{Nh}) \tag{40}$$

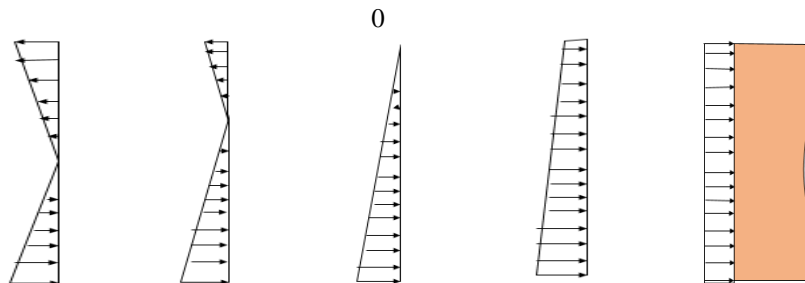


Fig. 2 Various linear forces factor

$$I = (I_0 + (\rho_{+h/2}^s + \rho_{-h/2}^s)) \quad (41)$$

Now, by applying Eringen nonlocal theory, the small scale effect on behavior of system will be investigated. Therefore, the strain-stress relations changes as

$$\sigma_{xx} - (e_0 a)^2 \frac{\partial^2 \sigma_{xx}}{\partial x^2} = E \varepsilon_{xx} \quad (42)$$

$$\sigma_{xz} - (e_0 a)^2 \frac{\partial^2 \sigma_{xz}}{\partial x^2} = G \gamma_{xz} \quad (43)$$

So, the strain-stress relations for an nanobeams which is made from viscoelastic functionally graded material can be shown as follows

$$\sigma_{xx} - \mu \frac{\partial^2 \sigma_{xx}}{\partial x^2} = E(z) \left(1 + g \frac{\partial^\alpha}{\partial t^\alpha}\right) \varepsilon_{xx} \quad (44)$$

$$\sigma_{xz} - \mu \frac{\partial^2 \sigma_{xz}}{\partial x^2} = G(z) \gamma_{xz} \quad (45)$$

By integrating above equations on the surface of the beam at the arbitrary point, the strain-force and strain-moment equations are obtained as follows

$$N - \mu \frac{\partial^2 N}{\partial x^2} = A_{xx} \frac{\partial u}{\partial x} + B_{xx} \frac{\partial \varphi}{\partial x} \quad (46)$$

$$M - \mu \frac{\partial^2 M}{\partial x^2} = B_{xx} \frac{\partial u}{\partial x} + D_{xx} \frac{\partial \varphi}{\partial x} \quad (47)$$

$$Q - \mu \frac{\partial^2 Q}{\partial x^2} = C_{xz} \left(\frac{\partial w}{\partial x} + \varphi\right) \quad (48)$$

Where the coefficients of shear planes are defined as follows

$$A_{xx} = \int_A (E(z) + E^s) \left(1 + g \frac{\partial^\alpha}{\partial t^\alpha}\right) dA \quad (49)$$

$$B_{xx} = \int_A (E(z) + E^s) \left(1 + g \frac{\partial^\alpha}{\partial t^\alpha}\right) z dA \quad (50)$$

$$D_{xx} = \int_A (E(z) + E^s)(1 + g \frac{\partial^\alpha}{\partial t^\alpha}) z^2 dA \tag{51}$$

$$C_{xz} = K_s \int_A (G(z) + G^s) dA \tag{52}$$

Second-order derivation of the motion equations generates the following equations

$$N = A_{xx} \frac{\partial u}{\partial x} + B_{xx} \frac{\partial \varphi}{\partial x} + \mu(I_0 \frac{\partial^3 u}{\partial x \partial t^2} + I_1 \frac{\partial^3 \varphi}{\partial x \partial t^2} - \frac{\partial f}{\partial x}) \tag{53}$$

$$M = B_{xx} \frac{\partial u}{\partial x} + D_{xx} \frac{\partial \varphi}{\partial x} + \mu(I_1 \frac{\partial^3 u}{\partial x \partial t^2} + I_2 \frac{\partial^3 \varphi}{\partial x \partial t^2} + I_0 \frac{\partial^2 w}{\partial t^2} - F) \tag{54}$$

$$Q = C_{xz} (\frac{\partial w}{\partial x} + \varphi) + \mu(I \frac{\partial^3 w}{\partial x \partial t^2} - \frac{\partial F}{\partial x}) \tag{55}$$

In the last step, by substituting the shear plane's coefficient into motion of equation, the governing equation of system extracted as follows

$$A_{xx} \frac{\partial^2 u}{\partial x^2} + B_{xx} \frac{\partial^2 \varphi}{\partial x^2} + \mu \left(I_0 \frac{\partial^4 u}{\partial t^2 \partial x^2} + I_1 \frac{\partial^4 \varphi}{\partial t^2 \partial x^2} - \frac{\partial^2 f}{\partial x^2} \right) - I_0 \frac{\partial^2 u}{\partial t^2} - I_1 \frac{\partial^2 \varphi}{\partial t^2} + f = 0 \tag{56}$$

$$C_{xz} (\frac{\partial^2 w}{\partial x^2} + \frac{\partial \varphi}{\partial x}) + \mu(I \frac{\partial^4 w}{\partial t^2 \partial x^2} - \frac{\partial^2 F}{\partial x^2}) - I \frac{\partial^2 w}{\partial t^2} + F = 0 \tag{57}$$

$$B_{xx} \frac{\partial^2 u}{\partial x^2} + D_{xx} \frac{\partial^2 \varphi}{\partial x^2} - C_{xz} (\frac{\partial w}{\partial x} + \varphi) + \mu(I_1 \frac{\partial^4 u}{\partial t^2 \partial x^2} + I_2 \frac{\partial^4 \varphi}{\partial t^2 \partial x^2}) - I_1 \frac{\partial^2 u}{\partial t^2} - I_2 \frac{\partial^2 \varphi}{\partial t^2} = 0 \tag{58}$$

3. Solution procedure

In order to predict solution of Eq. (58) semi-analytical approach can be applied all kind of boundary condition. In this paper, governing equation is solved by using the differential transformed method (DTM).

3.1 Differential transformed method (DTM)

The differential transformed method is a useful method for solving differential equations with least error which has the ability to solve nonlinear equations. Hassan (2002) applied the differential transformed method (DTM) to eigenvalue and by doing so, normalized the eigenfunctions. Wang (2013) investigated the axial vibration of a stepped bar consisting of two

uniform sections. In order to solve the dynamic equation, the differential transformation method is used. This method applies to a series of definitions to the governing equations and the boundary conditions that is the differential equations transformed to a series of algebraic equations.

Based on the function provided by Chen (2004) transformed equation if $f(x)$ can be represent as follows

$$F[k] = \frac{1}{k!} \left(\frac{d^k f(x)}{dx^k} \right)_{x=x_0} \quad (59)$$

Where, $f(x)$ and $F[k]$ shows main function and transformed equation respectively. The reverse transformed function is also indicated as follow

$$f(x) = \sum_{k=0}^{\infty} (x-x_0)^k F[k] \quad (60)$$

By combining the two above equation can be shown

$$f(x) = \sum_{k=0}^{\infty} \frac{(x-x_0)^k}{k!} \left(\frac{d^k f(x)}{dx^k} \right)_{x=x_0} \quad (61)$$

But in real use, series should be limited.

$$f(x) = \sum_{k=0}^N \frac{(x-x_0)^k}{k!} \left(\frac{d^k f(x)}{dx^k} \right)_{x=x_0} \quad (62)$$

With regardless of the limited point following relation can be achieved

$$f(x) = \sum_{k=N+1}^{\infty} \frac{(x-x_0)^k}{k!} \left(\frac{d^k f(x)}{dx^k} \right)_{x=x_0} \quad (63)$$

Table 1 A series of preset transformation rules (Chen 2004)

Original function	Transformed function
$f(x) = g(x) \pm h(x)$	$F(K) = G(K) \pm H(K)$
$f(x) = \lambda g(x)$	$F(K) = \lambda G(K)$
$f(x) = g(x)h(x)$	$F(K) = \sum_{l=0}^K G(K-l)H(l)$
$f(x) = \frac{d^n g(x)}{dx^n}$	$F(K) = \frac{(k+n)!}{k!} G(K+n)$
$f(x) = x^n$	$F(K) = \delta(K-n) = \begin{cases} 1 & k = n \\ 0 & k \neq n \end{cases}$

Table 2 A series of preset standard transmitted boundary condition rules (Chen 2004)

X = 0		X = L	
Original B.C.	Transformed B.C.	Original B.C.	Transformed B.C.
$f(0) = 0$	$F[0] = 0$	$f(L) = 0$	$\sum_{k=0}^{\infty} F[k] = 0$
$\frac{df(0)}{dx} = 0$	$\frac{dF[0]}{dx} = 0$	$\frac{df(L)}{dx} = 0$	$\sum_{k=0}^{\infty} k F[k] = 0$
$\frac{d^2f(0)}{dx^2} = 0$	$\frac{d^2F[0]}{dx^2} = 0$	$\frac{d^2f(L)}{dx^2} = 0$	$\sum_{k=0}^{\infty} k(k-1)F[k] = 0$
$\frac{d^3f(0)}{dx^3} = 0$	$\frac{d^3F[0]}{dx^3} = 0$	$\frac{d^3f(L)}{dx^3} = 0$	$\sum_{k=0}^{\infty} k(k-1)(k-2)F[k] = 0$

A series of transformations rules which are preset and have been recruited in the past research such as Chen (2004) are shown in the Table 1.

The standard boundary condition transmitted according to the differential transformed method are also shown in the Table 2.

By applying the above coefficient to the governing equations of system, algebraic equations of system's motion can be represents as follows

$$\begin{aligned}
 &A_{xx}(k+1)(k+2)U[k+2] + B_{xx}(k+1)(k+2)\phi[k+2] \\
 &- \mu(I_0\omega^2(k+1)(k+2)U[k+2] + I_1\omega^2(k+1)(k+2)\phi[k+2]) \\
 &+ I_0\omega^2U[k] + I_1\omega^2\phi[k] = 0
 \end{aligned} \tag{64}$$

$$C_{xz} \frac{(k+2)!}{k!}W[k+2] + (k+1)\phi[k+1] - \mu I \omega^2 \frac{(k+2)!}{k!}W[k+2] + I \omega^2W[k] = 0 \tag{65}$$

$$\begin{aligned}
 &B_{xx} \frac{(k+2)!}{k!}U[k+2] + D_{xx} \frac{(k+2)!}{k!}\phi[k+2] \\
 &- C_{xz}((k+2)!W[k+1] + \phi[k+2]) - \mu I_1 \omega^2 \frac{(k+2)!}{k!}U[k+2] \\
 &+ I_2 \omega^2W[k] \frac{(k+2)!}{k!}\phi[k+2] + I_1 \omega^2U[k] + I_2 \omega^2U\phi[k] = 0
 \end{aligned} \tag{66}$$

In which $U[k]$, $W[k]$ and $\phi[k]$ shows transformed function related to u , w and ϕ . According to the transformation rules which are related to the boundary conditions, simply-simply supported boundary condition, clamped-clamped boundary condition, clamped-simply supported boundary condition and cantilever boundary condition are shown in below equation respectively.

$$\begin{aligned}
 &W[0] = 0, \quad \phi[0] = 0, \quad U[0] = 0 \\
 &\sum_{i=0}^{\infty} W[k] = 0, \quad \sum_{i=0}^{\infty} k \phi[k] = 0, \quad \sum_{i=0}^{\infty} k U[k] = 0
 \end{aligned} \tag{67a}$$

$$\begin{aligned} W[0] = 0, \quad \varphi[0] = 0, \quad U[0] = 0 \\ \sum_{i=0}^{\infty} W[k] = 0, \quad \sum_{i=0}^{\infty} \varphi[k] = 0, \quad \sum_{i=0}^{\infty} U[k] = 0 \end{aligned} \quad (67b)$$

$$\begin{aligned} W[0] = 0, \quad \varphi[0] = 0, \quad U[0] = 0 \\ \sum_{i=0}^{\infty} W[k] = 0, \quad \sum_{i=0}^{\infty} k \varphi[k] = 0, \quad \sum_{i=0}^{\infty} k U[k] = 0 \end{aligned} \quad (67c)$$

$$\begin{aligned} W[0] = 0, \quad \varphi[0] = 0, \quad U[0] = 0 \\ \sum_{i=0}^{\infty} (k-2)(k-1)k W[k] = 0, \quad \sum_{i=0}^{\infty} k \varphi[k] = 0, \quad \sum_{i=0}^{\infty} k U[k] = 0 \end{aligned} \quad (67d)$$

Governing equation and related boundary condition can be written as eigen function problem as follows

$$\begin{bmatrix} A_{11}(\omega) & A_{12}(\omega) & A_{13}(\omega) \\ A_{21}(\omega) & A_{22}(\omega) & A_{23}(\omega) \\ A_{31}(\omega) & A_{32}(\omega) & A_{33}(\omega) \end{bmatrix} \begin{bmatrix} U \\ W \\ \phi \end{bmatrix} = 0 \quad (68)$$

Which matrix 3×3 describes coefficient of U , W and Φ , respectively. Hence, in order to find the answer of the system the coefficient's determinism must be zero.

$$\begin{vmatrix} A_{11}(\omega) & A_{12}(\omega) & A_{13}(\omega) \\ A_{21}(\omega) & A_{22}(\omega) & A_{23}(\omega) \\ A_{31}(\omega) & A_{32}(\omega) & A_{33}(\omega) \end{vmatrix} = 0 \quad (69)$$

4. Results and discussion

To verify the accuracy of calculated results which are extracted based on the differential transformed method (DTM), "reduce the problem condition to vibration analysis for simple Timoshenko nanobeam under simply supported boundary condition to be consistent with the Eltahir *et al.* (2014) research. The present results are compared with the results presented by Eltahir *et al.* (2014) for the natural frequency response of Timoshenko functionally graded nanobeam. The comparison results can be seen in Table 3 which shows a good agreement and verifies the presented approach. The FG nanobeam is supposed to be made of aluminum ($E = 70$ GPa) and alumina ($E = 380$ GPa) and subjected a uniformity distributed the normal load from $x = 0$ to $x = l_x$. In this case, the numerical loading factor is equal to zero at ($\chi = 0$). The nanobeam is rectangular with simply supported boundary condition along both edges. As given in Table 4, the linear fundamental natural frequency for simply supported boundary condition compared with Eltahir *et al.* (2014), "as it can be observed the results are in excellent agreement.

Table 3 Non-dimensional natural frequency comparison ($\bar{\omega}_1 = \omega_1 L^2 \sqrt{\rho A / EI}$) for Timoshenko nanobeam under simply supported boundary condition ($b = 1000$ nm, $L = 10,000$ nm, $h = 100$ nm, $p = 0$)

L/h	$\mu \times 10^{-12}$	Eltaher <i>et al.</i> (2014)	Present
			DTM
20	0	9.8797	9.8295
	1	9.4238	9.3776
	2	9.0257	8.9828
	3	8.6741	8.6341
	4	8.3607	8.3230
	5	8.0789	8.0433
50	0	9.8724	9.8631
	1	9.4172	9.4097
	2	9.0205	9.0135
	3	8.6700	8.6636
	4	8.3575	8.3514
	5	8.0765	8.0707
100	0	9.8700	9.8679
	1	9.4162	9.4143
	2	9.0197	9.0180
	3	8.6695	8.6678
	4	8.3571	8.3555
	5	8.0762	8.0747

Table 4 Comparison of non-dimensional frequency for FG-nanobeam

$\mu \times 10^{-9}$	$k = 0$		$k = 1$		$k = 2$		$k = 5$	
	Eltaher <i>et al.</i> 2012	Present	Eltaher <i>et al.</i> 2012	Present	Eltaher <i>et al.</i> 2012	Present	Eltaher <i>et al.</i> 2012	Present
0	9.8724	9.8679	7.0852	6.9951	6.5189	6.4225	5.9990	5.9421
1	9.4172	9.4143	6.7583	6.6736	6.2191	6.1272	5.7218	5.6690
2	9.0205	9.0180	6.4737	6.3926	5.9571	5.8693	5.4808	5.4303
3	8.6700	8.6678	6.2222	6.1444	5.7257	5.6414	5.2679	5.2195

The nonlocal parameter (μ) effect on non-dimensional frequency for various boundary condition in various aspect ratio shown in Figs. 3 to 5. These figures illustrates, the non-dimensional frequency decreases by an increase in the value of the nonlocal parameter from 0 to 10. The effects of various aspect ratio in the frequency of system increases by the increase in the value of aspect ratio. The amount of non-dimensional frequency in the various amount of aspect ratio has a large difference with each other. When the nanobeam is too narrow, beam's stability disappears.

The effect of various boundary condition on non-dimensional frequency in different aspect ratio can be understandable from the mentioned figures. The amount of the non-dimensional frequency in simply supported boundary condition represents a greater amount than the non-

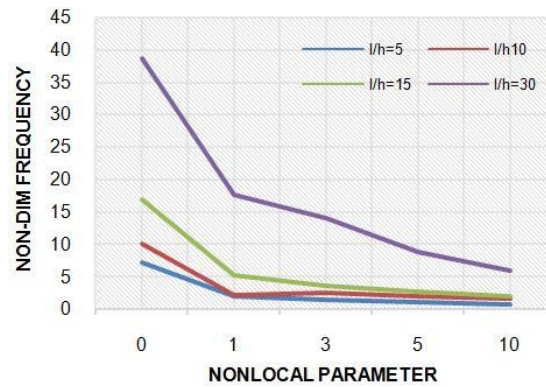


Fig. 3 Nonlocal coefficient effect on vibration behavior of system under s-s boundary condition for various aspect ratio ($U = 10, \Delta T = 25$ & $K_G = 10$)

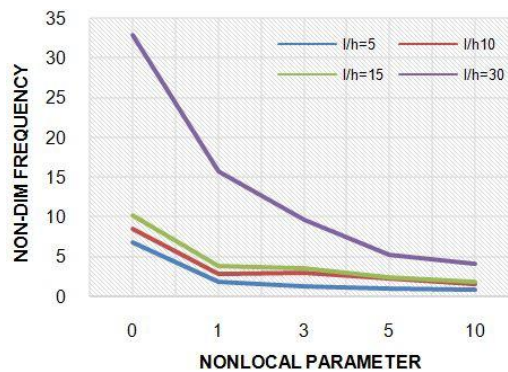


Fig. 4 Nonlocal coefficient effect on vibration behavior of system under c-c boundary condition for various aspect ratio ($U = 10, \Delta T = 25$ & $K_G = 10$)

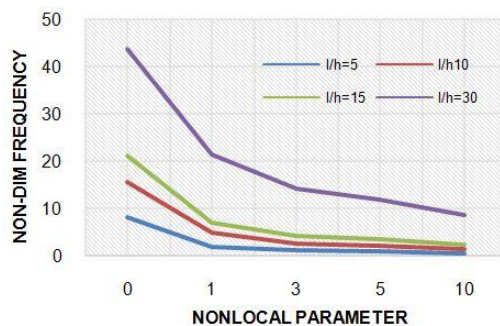


Fig. 5 Nonlocal coefficient effect on vibration behavior of system under cantilever boundary condition for various aspect ratio ($U = 10, \Delta T = 25$ & $K_G = 10$)

dimensional frequency in the clamped boundary condition. And also, the amount of the non-dimensional frequency in simply supported boundary condition represents a smaller amount than non-dimensional frequency in cantilever boundary condition. This behavior of the system was fairly predictable beforehand.

To illustrate the effect of FG index on the non-dimensional frequency of nanobeams, the variation of non-dimensional frequency with FG index in various aspect ratios are presented in Figs. 6-8. According to these figures, it can be concluded that, the FG index effects are nearly lost to low aspect ratio in all cases. This is predictable because of the effect of FG index increases by the increase in structure's aspect ratio. Furthermore, the gap between the amounts in different aspect ratio increase by the increase in FG index. Anyway, it is realized that, the amount of non-dimensional frequency increases by increase in FG index although, this increase in low aspect ratio is not very tangible.

Fig. 9 shows the effect of thermal environment on non-dimensional frequency in the various boundary condition. This figure shows, the frequency increases when the nanobeam placed in higher temperature environment, especially for cantilever boundary condition. The effects of thermal environment on non-dimensional frequency increases for the higher value of thermal

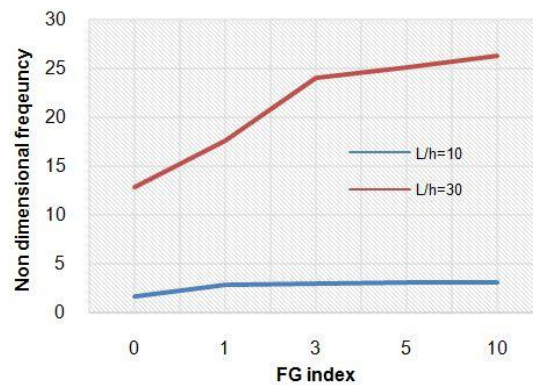


Fig. 6 FG index effect on vibration behavior of system under s-s boundary condition for various aspect ratio ($\mu = 1 \times 10^{-9}$, $\Delta T = 25$ & $K_G = 10$)

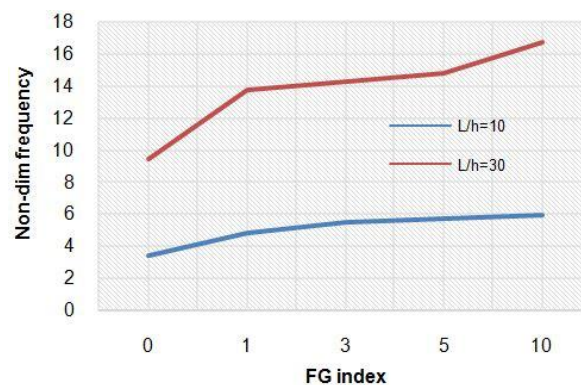


Fig. 7 FG index effect on vibration behavior of system under c-c boundary condition for various aspect ratio ($\mu = 1 \times 10^{-9}$, $\Delta T = 25$ & $K_G = 10$)

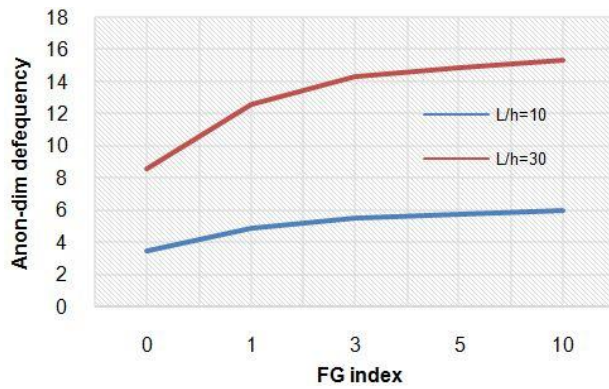


Fig. 8 FG index effect on vibration behavior of system under cantilever boundary condition for various aspect ratio ($\mu = 1 \times 10^{-9}$, $\Delta T = 25$ & $K_G = 10$)

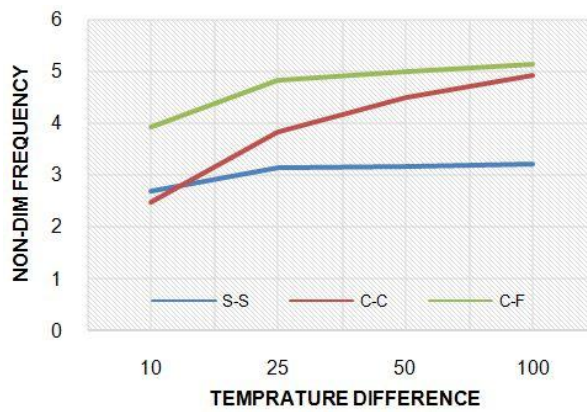


Fig. 9 Thermal environment effect on vibration behavior of system under various boundary condition ($\mu = 1 \times 10^{-9}$, $L/h = 10$ & $K_G = 10$)



Fig. 10 Frictional order effect on vibration behavior of system under various boundary condition ($\mu = 1 \times 10^{-9}$, $L/h = 10$, $g = 0.05$ & $K_G = 10$)

changes. For more information, the difference between frequencies of the system simply supported boundary condition is not tangible by an increase in thermal changes. Fig. 10 shows the effect of the frictional order of viscoelastic material on the non-dimensional frequency of various boundary condition. According to the figure, non-dimensional frequency decrease by the increase in viscoelastic frictional order. It is predictable because increase in the frictional order of material that subjected to the in-plane loading causes material become more flexible. The effects of frictional order on non-dimensional frequency more decreases for simply supported boundary condition.

Table 5 shows the effect of Pasternak medium on non-dimensional buckling of FG nanobeams for various boundary condition. The results show that the frequency increases by the increase in the amount of Pasternak coefficient. This behavior is visible for all of cases and also, the beam's frequency shows more increases for cantilever boundary condition. The important note in this table is the difference in the value of frequency between simply supported boundary condition and cantilever boundary condition.

Table 6 Shows the effect of residual surface stresses effect on the frequency of nanobeam. Non-dimensional frequency in the FGM nanobeam increases in the presence of residual surface stresses. The fundamental frequency increases significantly for cantilever boundary condition. These behavior occurs on the nanobeams because the degree of freedom in cantilever beams causes increases the impact of the beam on vibration behavior from external forces.

Table 5 Pasternak foundation effect on vibration behavior of system under various boundary condition ($\mu = 1 \times 10^{-9}$, $L/h = 10$, $g = 0.05$ & $u = 1$)

K_G	S-S	C-C	C-F
0	2.6834	4.8204	4.9205
5	3.1118	6.1219	6.7179
10	3.1235	6.7315	6.9232

Table 6 Residual Surface stresses effect on vibration behavior of system under various boundary condition ($\mu = 1 \times 10^{-9}$, $L/h = 10$, $g = 0.05$ & $u = 1$)

$H = 2b\tau_0$	S-S	C-C	C-F
0	2.7101	3.4394	4.0017
$2b\tau_0$	3.1235	4.8204	4.9205

Table 7 The effect of different linear varying load on vibration behavior of system under various FG index and various nonlocal parameter ($\gamma = 0.4 \times 10^{-9}$)

	$\chi = 0$	$\chi = 0.5$	$\chi = 1$	$\chi = 1.5$	$\chi = 2$	
k	0	3.5623	2.1798	2.1518	1.8580	1.9770
	1	4.2106	3.8328	3.1801	2.6981	2.9075
	3	4.7552	4.5985	3.6655	3.6646	3.8393
μ	1	2.6896	3.0328	3.1801	2.6981	2.9075
	3	2.3615	2.5924	2.8213	2.1259	2.6285
	5	1.7327	1.9415	2.4463	2.2886	2.3317

Table 7 shows the effect of various linearly loading factors on the frequency of nanobeam. Non-dimensional frequency in the FGM nanobeam decreases by an increase in linear loading factors from 0 (pure pressure) to 2 (pure bending), “This increases in more tangible for a pure bending state. The fundamental frequency increases significantly by an increase in FG index in presence of various loading factor.

Table 8 shows the effect of humidity percent on the frequency of nanobeam. Non-dimensional frequency in the FGM nanobeam decreases in the presence of humidity environment and this behavior was predictable because humidity environment causes the material becomes more flexible. And also non-dimensional frequency decreases by an increase in the nonlocal parameter. This behavior occurs in all cases. As well as the frequency of nanobeam decreases by the increase in FG index amount. The presences of humidity environment lead to further decrease in frequency by the increase in FG indexes and nonlocal parameter.

Table 8 The effect of different humidity percent on vibration behavior of system under various boundary condition, nonlocal parameter and FG indexes ($L = 10 \text{ nm}$, $h = L/20$, $b = 0.5h$, $\Delta T = 10^\circ\text{C}$)

$\mu \text{ *nm}^2$	% ΔH	$k = 0.1$			$k = 1$		
		$V = -0.5$	$V = 0$	$V = 0.5$	$V = -0.5$	$V = 0$	$V = 0.5$
S-S							
0	0	9.12949	9.0449	8.9595	7.0327	6.9356	6.8370
	10	9.1177	9.0330	8.9475	6.9695	6.8714	6.7720
	20	9.1059	9.0211	8.9555	6.9057	6.8067	6.7063
2	0	8.3280	8.2352	8.1413	6.4140	6.3074	6.1989
	10	8.3151	8.2222	8.1282	6.3447	6.2368	6.1271
	20	8.3022	8.2091	8.1150	6.2745	6.1655	6.0544
C-S							
0	0	14.3275	14.2648	14.2018	11.0425	10.9706	10.8981
	10	14.3187	14.2560	14.1929	10.9956	10.9234	10.8506
	20	14.3100	14.2472	14.1841	10.9486	10.8760	10.8029
2	0	12.8872	12.8068	12.7258	9.9305	9.8382	9.7450
	10	12.876	12.7955	12.7145	9.8704	9.7775	9.6837
	20	12.8648	12.7842	12.7032	9.8099	9.7164	9.6220
C-C							
0	0	20.8331	20.7871	20.7410	16.0601	16.0074	15.9545
	10	20.8267	20.7807	20.7345	16.0258	15.9729	15.9198
	20	20.8203	20.7742	20.7281	15.9913	15.9383	15.8851
2	0	18.6089	18.5336	18.4580	14.3427	14.2564	14.1695
	10	18.5984	18.5231	18.4474	14.2864	14.1998	14.1126
	20	18.5879	18.5125	18.4368	14.2300	14.1430	14.0554

5. Conclusions

A general view of the article contains a lot of content, including the importance of temperature raises, Pasternak foundation, size dependent effect, humidity environment, residual surface stress and etc. on the frequency response of functionally graded nanobeams that subjected to linear in-plane load based on elasticity nonlocal theory. The governing equation is solved by using the differential transformed method. The results are compared with the results that are extracted by Eltahir *et al.* (2014) and shows good agreement with them. Various boundary condition is considered for the FGM nanobeam. According to the results it can be seen that, Pasternak foundation causes an increase in frequency for various loading condition. The non-dimensional frequency increases for the higher value of nanobeams temperature. Responses of non-dimensional frequency are lesser than local states for various loading condition in all cases. In addition, the frequency of system decreases for higher value of nonlocal parameter. The non-dimensional frequency increases by an increase in the value of FG index. For the special state, when loading condition makes pure in-plane bending, the effect of nonlocal is most important than other states. Anyway, at the huge beams the difference in the small scale effect is negligible, however, there is the difference between bending state and other states even for large dimension. It can be seen that, frequency decreases by an increase in the humidity percent. Further, the effect of small scale effect increases for the higher value of mode number. By increase in the FG index at linear loading factors, the amount of beams frequency increases by the increase in the value of nonlocal parameter or aspect ratio, the amount of beams frequency reduced r in linear load factor.

References

- Ansari, R., Oskouie, M.F. and Gholami, R. (2016), "Size-dependent geometrically nonlinear free vibration analysis of fractional viscoelastic nanobeams based on the nonlocal elasticity theory", *Phys. E: Low-dimens. Syst. Nanostruct.*, **75**, 266-271.
- Arda, M. and Aydogdu, M. (2017), *Longitudinal Vibration of CNTs Viscously Damped in Span*.
- Barooti, M.M., Safarpour, H. and Ghadiri, M. (2017), "Critical speed and free vibration analysis of spinning 3D single-walled carbon nanotubes resting on elastic foundations", *Eur. Phys. J. Plus*, **132**(1), 6.
- Chen, S.S. (2004), "Application of the differential transformation method to a non-linear conservative system", *Appl. Math. Computat.*, **154**(2), 431-441.
- Duan, K., Li, Y., Li, L., Hu, Y. and Wang, X. (2018), "Diamond nanothread based resonators: ultrahigh sensitivity and low dissipation", *Nanoscale*, **10**(17), 8058-8065.
- Ebrahimi, F. and Barati, M.R. (2016a), "Temperature distribution effects on buckling behavior of smart heterogeneous nanosize plates based on nonlocal four-variable refined plate theory", *Int. J. Smart Nano Mater.*, 1-25.
- Ebrahimi, F. and Barati, M.R. (2016b), "Vibration analysis of smart piezoelectrically actuated nanobeams subjected to magneto-electrical field in thermal environment", *J. Vib. Control*, 1077546316646239.
- Ebrahimi, F. and Barati, M.R. (2016c), "Size-dependent thermal stability analysis of graded piezomagnetic nanoplates on elastic medium subjected to various thermal environments", *Appl. Phys. A*, **122**(10), 910.
- Ebrahimi, F. and Barati, M.R. (2016d), "Static stability analysis of smart magneto-electro-elastic heterogeneous nanoplates embedded in an elastic medium based on a four-variable refined plate theory", *Smart Mater. Struct.*, **25**(10), 105014.
- Ebrahimi, F. and Barati, M.R. (2016e), "Buckling analysis of piezoelectrically actuated smart nanoscale plates subjected to magnetic field", *J. Intel. Mater. Syst. Struct.*, 1045389X16672569.
- Ebrahimi, F. and Barati, M.R. (2016f), "A nonlocal higher-order shear deformation beam theory for

- vibration analysis of size-dependent functionally graded nanobeams”, *Arab. J. Sci. Eng.*, **41**(5), 1679-1690.
- Ebrahimi, F. and Barati, M.R. (2016g), “Vibration analysis of nonlocal beams made of functionally graded material in thermal environment”, *Eur. Phys. J. Plus*, **131**(8), 279.
- Ebrahimi, F. and Barati, M.R. (2016h), “Dynamic modeling of a thermo-piezo-electrically actuated nanosize beam subjected to a magnetic field”, *Appl. Phys. A*, **122**(4), 1-18.
- Ebrahimi, F. and Barati, M.R. (2016i), “A unified formulation for dynamic analysis of nonlocal heterogeneous nanobeams in hygro-thermal environment”, *Appl. Phys. A*, **122**(9), 792.
- Ebrahimi, F. and Barati, M.R. (2016j), “A nonlocal higher-order refined magneto-electro-viscoelastic beam model for dynamic analysis of smart nanostructures”, *Int. J. Eng. Sci.*, **107**, 183-196.
- Ebrahimi, F. and Barati, M.R. (2017), “A third-order parabolic shear deformation beam theory for nonlocal vibration analysis of magneto-electro-elastic nanobeams embedded in two-parameter elastic foundation”, *Adv. Nano Res., Int. J.*, **5**(4), 313-336.
- Ebrahimi, F. and Barati, M.R. (2018), “Stability analysis of functionally graded heterogeneous piezoelectric nanobeams based on nonlocal elasticity theory”, *Adv. Nano Res., Int. J.*, **6**(2), 93-112.
- Ebrahimi, F. and Dabbagh, A. (2016), “On flexural wave propagation responses of smart FG magneto-electro-elastic nanoplates via nonlocal strain gradient theory”, *Compos. Struct.*, **162**, 281-293.
- Ebrahimi, F. and Farazmandnia, N. (2017), “Thermo-mechanical vibration analysis of sandwich beams with functionally graded carbon nanotube-reinforced composite face sheets based on a higher-order shear deformation beam theory”, *Mech. Adv. Mater. Struct.*, **24**(10), 820-829.
- Ebrahimi, F. and Habibi, S. (2017), “Low-velocity impact response of laminated FG-CNT reinforced composite plates in thermal environment”, *Adv. Nano Res., Int. J.*, **5**(2), 69-97.
- Ebrahimi, F. and Haghi, P. (2018), “Wave dispersion analysis of rotating heterogeneous nanobeams in thermal environment”, *Adv. Nano Res., Int. J.*, **6**(1), 21-37.
- Ebrahimi, F. and Hosseini, S.H.S. (2016a), “Thermal effects on nonlinear vibration behavior of viscoelastic nanosize plates”, *J. Therm. Stress.*, **39**(5), 606-625.
- Ebrahimi, F. and Hosseini, S.H.S. (2016b), “Double nanoplate-based NEMS under hydrostatic and electrostatic actuations”, *Eur. Phys. J. Plus*, **131**(5), 1-19.
- Ebrahimi, F. and Mahmoodi, F. (2018), “Vibration analysis of carbon nanotubes with multiple cracks in thermal environment”, *Adv. Nano Res., Int. J.*, **6**(1), 57-80.
- Ebrahimi, F. and Shaghaghi, G.R. (2015), “Vibration analysis of an initially pre-stressed rotating carbon nanotube employing differential transform method”, *Int. J. Adv. Des. Manuf. Technol.*, **8**(4), 13-21.
- Ebrahimi, F. and Shaghaghi, G.R. (2016), “Thermal effects on nonlocal vibrational characteristics of nanobeams with non-ideal boundary conditions”, *Smart Struct. Syst., Int. J.*, **18**(6), 1087-1109.
- Ebrahimi, F. and Shaghaghi, G.R. (2018), “Nonlinear vibration analysis of electro-hygro-thermally actuated embedded nanobeams with various boundary conditions”, *Microsyst. Technol.*, **24**(12), 5037-5054.
- Ebrahimi, F., Shaghaghi, G.R. and Salari, E. (2014), “Vibration analysis of size-dependent nano beams based on nonlocal timoshenko beam theory”, *J. Mech. Eng. Technol. (JMET)*, **6**(2).
- Ebrahimi, F., Boreiry, M. and Shaghaghi, G. (2015), “Investigating the surface elasticity and tension effects on critical buckling behaviour of nanotubes based on differential transformation method”, *J. Mech. Eng. Technol. (JMET)*, **7**(1).
- Ebrahimi, F., Barati, M.R. and Dabbagh, A. (2016a), “A nonlocal strain gradient theory for wave propagation analysis in temperature-dependent inhomogeneous nanoplates”, *Int. J. Eng. Sci.*, **107**, 169-182.
- Ebrahimi, F., Shaghaghi, G.R. and Boreiry, M. (2016b), “A semi-analytical evaluation of surface and nonlocal effects on buckling and vibrational characteristics of nanotubes with various boundary conditions”, *Int. J. Struct. Stabil. Dyn.*, **16**(6), 1550023.
- Ebrahimi, F., Salari, E. and Hosseini, S.A.H. (2016c), “In-plane thermal loading effects on vibrational characteristics of functionally graded nanobeams”, *Meccanica*, **51**(4), 951-977.
- Ebrahimi, F., Ehyaei, J. and Babaei, R. (2016d), “Thermal buckling of FGM nanoplates subjected to linear and nonlinear varying loads on Pasternak foundation”, *Adv. Mater. Res., Int. J.*, **5**(4), 245-261.

- Ebrahimi, F., Babaei, R. and Shaghghi, G.R. (2018), "Nonlocal buckling characteristics of heterogeneous plates subjected to various loadings", *Adv. Aircr. Spacecr. Sci.*, **5**(5), 515-531.
- Ehyaiei, J., Ebrahimi, F. and Salari, E. (2016), "Nonlocal vibration analysis of FG nano beams with different boundary conditions", *Adv. Nano Res., Int. J.*, **4**(2), 85-111.
- Ehyaiei, J., Akbarshahi, A. and Shafiei, N. (2017), "Influence of porosity and axial preload on vibration behavior of rotating FG nanobeam", *Adv. Nano Res., Int. J.*, **5**(2), 141-169.
- Elishakoff, I., Challamel, N., Soret, C., Bekel, Y. and Gomez, T. (2013), "Virus sensor based on single-walled carbon nanotube: improved theory incorporating surface effects", *Phil. Trans. R. Soc. A*, **371**(1993), 20120424.
- Eltaher, M.A., Khairy, A., Sadoun, A.M. and Omar, F.A. (2014), "Static and buckling analysis of functionally graded Timoshenko nanobeams", *Appl. Math. Comput.*, **229**, 283-295.
- Eringen, A.C. (1983), "On differential equations of nonlocal elasticity and solutions of screw dislocation and surface waves", *J. Appl. Phys.*, **54**(9), 4703-4710.
- Eringen, A.C. and Edelen, D.G.B. (1972), "On nonlocal elasticity", *Int. J. Eng. Sci.*, **10**(3), 233-248.
- Fernandes, R., El-Borgi, S., Mousavi, S.M., Reddy, J.N. and Mechmoum, A. (2017), "Nonlinear size-dependent longitudinal vibration of carbon nanotubes embedded in an elastic medium", *Physica E: Low-dimens. Syst. Nanostruct.*, **88**, 18-25.
- Ghadiri, M., Ebrahimi, F., Salari, E., Hosseini, S.A.H. and Shaghghi, G.R. (2015), "Electro-thermo-mechanical vibration analysis of embedded single-walled boron nitride nanotubes based on nonlocal third-order beam theory", *Int. J. Multiscale Computat. Eng.*, **13**(5).
- Hassan, I.A.H. (2002), "On solving some eigenvalue problems by using a differential transformation", *Appl. Math. Comput.*, **127**(1), 1-22.
- Hwang, H.J., Jung, S.L., Cho, K.H., Kim, Y. and Jang, H. (2010), "Tribological performance of brake friction materials containing carbon nanotubes", *Wear*, **268**(3-4), 519-525.
- Ju, S.P. (2004), "Application of differential transformation to transient advective-dispersive transport equation", *Appl. Math. Comput.*, **155**(1), 25-38.
- Karličić, D., Kozić, P., Adhikari, S., Cajić, M., Murmu, T. and Lazarević, M. (2015), "Nonlocal mass-nanosensor model based on the damped vibration of single-layer graphene sheet influenced by in-plane magnetic field", *Int. J. Mech. Sci.*, **96**, 132-142.
- Li, L. and Hu, Y. (2017), "Post-buckling analysis of functionally graded nanobeams incorporating nonlocal stress and microstructure-dependent strain gradient effects", *Int. J. Mech. Sci.*, **120**, 159-170.
- Li, X.F., Tang, G.J., Shen, Z.B. and Lee, K.Y. (2015), "Resonance frequency and mass identification of zeptogram-scale nanosensor based on the nonlocal beam theory", *Ultrasonics*, **55**, 75-84.
- Marzbanrad, J., Ebrahimi-Nejad, S., Shaghghi, G. and Boreiry, M. (2018b), "Nonlinear vibration analysis of piezoelectric functionally graded nanobeam exposed to combined hygro-magneto-electro-thermo-mechanical loading", *Mater. Res. Express*, **5**(7), 075022.
- Miller, R.E. and Shenoy, V.B. (2000), "Size-dependent elastic properties of nanosized structural elements", *Nanotechnology*, **11**(3), 139.
- Mohammadimehr, M., Mohammadi-Dehabadi, A.A. and Maraghi, Z.K. (2017), "The effect of non-local higher order stress to predict the nonlinear vibration behavior of carbon nanotube conveying viscous nanoflow", *Phys. B: Condensed Matter*, **510**, 48-59.
- Mori, T. and Tanaka, K. (1973), "Average stress in matrix and average elastic energy of materials with misfitting inclusions", *Acta metallurgica*, **21**(5), 571-574.
- Murmu, T. and Adhikari, S. (2013), "Nonlocal mass nanosensors based on vibrating monolayer graphene sheets", *Sensors Actuators B: Chem.*, **188**, 1319-1327.
- Pradhan, S.C. and Phadikar, J.K. (2011), "Nonlocal theory for buckling of nanoplates", *Int. J. Struct. Stabil. Dyn.*, **11**(3), 411-429.
- Wang, Z.G. (2013), "Axial vibration analysis of stepped bar by differential transformation method", In: *Applied Mechanics and Materials* (Vol. 419, pp. 273-279), Trans Tech Publications.
- Wu, H.L., Yang, J. and Kitipornchai, S. (2016), "Nonlinear vibration of functionally graded carbon nanotube-reinforced composite beams with geometric imperfections", *Compos. Part B: Eng.*, **90**, 86-96.

- Zhou, C.W., Sun, X.K., Lainé, J.P., Ichchou, M.N., Zine, A., Hans, S. and Boutin, C. (2018), “Wave Propagation Feature in Two-Dimensional Periodic Beam Lattices with Local Resonance by Numerical Method and Analytical Homogenization Approach”, *Int. J. Appl. Mech.*, 1850042.
- Zhu, X. and Li, L. (2017), “On longitudinal dynamics of nanorods”, *Int. J. Eng. Sci.*, **120**, 129-145.

CC